

# Deep CNN based MR image denoising for tumor segmentation using watershed transform

Ghazanfar Latif<sup>\*1,2</sup>, D.N.F. Awang Iskandar<sup>1</sup>, Jaafar Alghazo<sup>2</sup>, Mohsin Butt<sup>3</sup>, Adil H. Khan<sup>1,4</sup>

<sup>1</sup> Faculty of Computer Science and Information Technology, Universiti Malaysia Sarawak, Malaysia.

<sup>2</sup> College of Computer Engineering and Sciences, Prince Mohammad bin Fahd University, Saudi Arabia.

<sup>3</sup> College of Applied and Supporting Studies, King Fahd University of Petroleum and Minerals, Saudi Arabia.

<sup>4</sup> College of Engineering, Prince Mohammad bin Fahd University, Saudi Arabia

\*Corresponding author E-mail: [glatif@pmu.edu.sa](mailto:glatif@pmu.edu.sa)

## Abstract

Magnetic Resonance Imaging (MRI) is considered one of the most effective imaging techniques used in the medical field for both clinical investigation and diagnosis. This is due to the fact that MRI provides many critical features of the tissue including both physiological and chemical information. Rician noise affects MR images during acquisition thereby reducing the quality of the image and complicating the accurate diagnosis. In this paper, we propose a novel technique for MR image denoising using Deep Convolutional Neural Network (Deep CNN) and anisotropic diffusion (AD) which we will refer to as Deep CNN-AD. Watershed transform is then used to segment the tumorous portion of the denoised image. The proposed method is tested on the BraTS MRI datasets. The proposed denoising method produced better results compared to previous methods. As denoising process affect the segmentation process therefore better denoised images by proposed technique produced more accurate segmentation with an average Specificity of 99.85% and dice coefficient of 90.46% thus indicating better performance of proposed technique.

**Keywords:** Deep CNN Denoising, Brain Tumor Segmentation, Anisotropic Diffusion, BraTS MRI, Rician Noise.

## 1. Introduction

Magnetic Resonance (MR) image is an effective, non-invasive imaging method to capture and analyse different body tissues which helps the physician to diagnose and cure the disease. Brain is the most critical and complicated part of the human body and relatively advanced techniques are required to observe the internal parts and tissues of it. The most common technique used by doctors for the diagnosis and treatment of tumors is the MR Imaging (MRI) Technique.

Two main types of tumors exist namely the primary brain tumor and secondary brain tumor. Primary brain tumor which is also known as malignant tumor; it is usually formed inside brain nerves [1]. Secondary brain tumor is originated from any other body part but spread through to the brain, e.g. tumor in lungs or breast spreading through to the brain causing secondary brain tumor [2]. Primary brain tumor has two main types. First one is malignant gliomas, which is generated inside glial cells of central nervous system and this is the most deadly brain tumor type [3]. Second type is Non-gliomas which does not arise from glial cells therefore it is considered as less dangerous compare to malignant gliomas [4]. Both types of tumor have different type of curing procedures and it is very critical for the doctors to identify the correct tumor type. In the presence of noise, the task of tumor classification is extremely difficult; therefore de-noising the MR image is very important and crucial to identify the correct brain tumor type.

Images of the brain internal structure and tissues are generated by powerful magnetic field in MR imaging technology. Noise is gen-

erated during the image acquisition and transmission phase. Thermal noise fluctuating the image in a random manner is generated due to magnetic field. Impulse noise is also observed during acquisition and transmission. These noise factors can affect the features of the MR images which are necessary in the classification of tumor type [5]. Minute variation of pixel intensity exist in grayscale image making the segmentation task a complex problem. Therefore, noise reduction in pre-processing stage, from MR images is pivotal. Besides thermal and impulse noise, there are other noises included in MR images, such as Speckle noise, Gaussian noise, Salt and Pepper noise and Rician distribution noise of MR images. Different filters and methods are used to suppress such noise types [6-7].

A number of methods for brain segmentation has been proposed and research work on this topic is still ongoing to design an automated system. Methods like Deep Convolution Neural Networks (CNN), Water shed transformation, and many other techniques has been used in this area [8-9].

The main motivation for this work is to enhance the automated accurate segmentation of the tumorous portion of MR images. Accurate segmentation and subsequent classification of tumorous image assists in the automated accurate diagnosis of tumor classes which affects the medication process and could lead to live saving applications. The accurate segmentation is directly affected by the quality of the MR images. Unfortunately, MR image get affected by noise during the image acquisition and transmission phase. Denoising the images sometimes degrades the quality of the image increasing the complexity of the segmentation. We propose in this paper a novel and simple denoising technique that results in de-

noising the image while maintaining the quality and key features of the image. The main contribution of this work is the proposal of a novel method for the effective denoising of the MR image using Deep CNN-AD. The proposed method maintains the quality of the image and the key features in the denoising process. This has significant effect in the effective and accurate segmentation of the tumor portion of the image.

In rest of the paper, section 2 presents the related work, section 3 details the proposed method, section 4 highlights the results and discussion, section 5 conclude the work and section 6 lists the references.

## 2. Related Work

Non-linear and linear denoising methods are used for MR image denoising. The linear filtering process is achieved by suppressing the noise through updating values of the pixel over the weighted average of adjacent pixels. This method is effective in noise reduction but image quality is degraded. The non-linear filtering process affects the images negatively yet preserving the image edges [10]. There are advantages and disadvantages for these methods for example the advantage of the Anisotropic Diffusion Filtering (ADF) is that it denoises even the smallest features of MR images and preserves the edge details but the downside to this method is that the adjustment of parameter number of iteration is very critical which can change the results completely [11-12]. Denoising methods based on Wavelet transformation, makes the scaling coefficient biased. Chi-square distribution technique is applied to make the coefficients independent from the signal [13]. Still it carries problems such as thresholding of the wavelets and scale assurance. In [14], the average of pixels local in feature space are calculated using non-local filtering method. Better results were achieved at the cost of higher computations. In [15], the authors proposed Bilateral Filtering (BF) based on the concept of domain filtering to preserve contour information. This method is also non-iterative in nature, which gives it an edge over ADF. The performance of non-local filtering can be improved by the technique used in BF; in which the new value of the pixel is calculated by using narrow spatial window thus preserving the large scale structures [16].

The most common method for MRI denoising is the Gaussian filter however this technique results in a blurry degrades image quality. Linear Minimum Mean Square Error (LMMSE) is used to estimate the Rician noise and due to powerful statistical approach of LMMSE the restoration of MR images improved but at the cost of higher computation [17]. A technique based on block wise comparison is exploited in [18] to remove the Rician noise. An algorithm named Low Rank Tensor Estimator (LRTE) is used as well for the process of denoising and showed better performance over many state of the art techniques. This algorithm was not efficient in real life problems because of the nuclear norm minimization in LRTE that ends up treating all singular values equally [19]. In [20], fuzzy logic incorporated with Non-Local Mean (NLM) to remove Rician noise by finding non-local homogenous pixels and eliminate the noise but this method was unable to preserve the edges efficiently.

CNN based segmentation methods solve the problem in a more natural way. In [21] basic CNN model is used to predict the value for each pixel and this prediction improves further once previous predicted values are given as input to the second CNN model. Multi-modal based CNN is proposed in [22], where processing is done at different distinct models and prediction is made after integration of the information from all the CNN models. In this method, a global super pixel segmentation is used at the end in order to ensure smooth segmentation process. In [23], same global supervision technique is incorporated with convolution at each stage of the network. Another CNN based method is proposed in [24], where both global and local contextual features are used and to speed up the process; convolution is implemented at final layer.

Watershed transformation is also one of most commonly used methods used for segmentation in which each image pixel is considered as height of a topographical relief and analogy of rain water forming lakes (referred to as catchment basins) are used to locate the boundaries at high gradient areas of the image [25].

## 3. Proposed Method

In this research paper, we propose a multi-step technique for MR Image denoising and smoothing with an enhanced brain tumor segmentation. In the pre-processing phase, initially the input MR image is denoised using the deep CNN method. To further reduce the noise in the image, anisotropic diffusion method is applied. 2-Dimensional Fast Fourier Transform (2D FFT) is then applied to the image to convert it in to frequency domain. The centre of spectrum is occupied with the zero-frequency component and a frequency cut off value depending on the average of the frequency components of the image is used to define a Gaussian low pass filter that smooths the input MR image and remove the irrelevant details. The image is then converted back to its time domain representation by applying the inverse Fast Fourier Transform (iFFT). The gradient magnitude is used as the segmentation function on which the watershed transform is applied for the tumor segmentation. The proposed technique is depicted in Fig. 1.

Rician noise produced from the original frequency domain measurements (complex Gaussian noise) to corrupt the MR Image [26]. The Rician probability density function  $p(x)$  for the noised image is calculated according to equation 1.

$$p(x) = \frac{x}{\sigma^2} \exp\left(-\frac{x^2 - A^2}{2\sigma^2}\right) I_0\left(\frac{x A}{\sigma^2}\right) \quad (1)$$

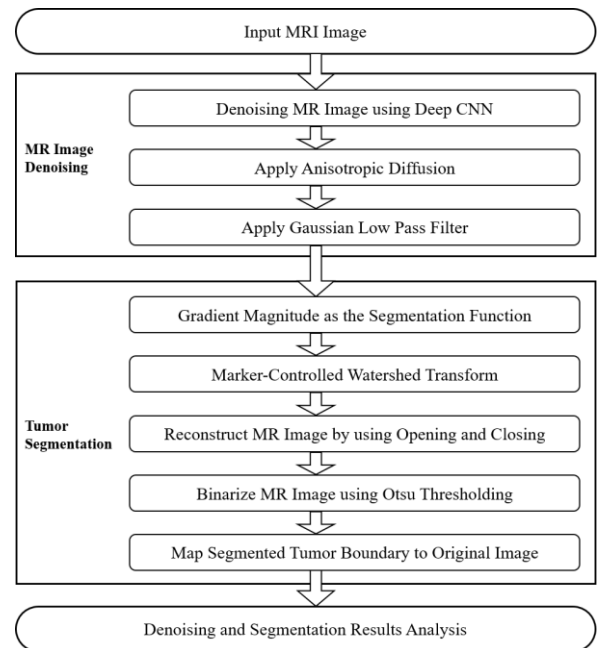


Fig. 1: Workflow of the Proposed Method

### 2.1. MR Image Denoising using Deep CNN

Deep Learning Convolutional Neural Networks are gaining fast popularity in various fields of image processing. Image denoising is a critical process in the image processing field. Image denoising refers to the practice of eradicating the noise from the corrupt image while maintaining the key features. The observed image in most image processing problems are affected by a degradation function and additive noise.

$$I'(n, m) = I(n, m) + a(n, n) \quad (2)$$

Where  $I'(n, m)$  refers to the observed image,  $I(n, m)$  is the original image,  $a(n, m)$  is the additive noise. Traditional methods used in image processing cannot fully remove the noised out pixels from the original image. Deep CNNs can help in this regard by learning the key features that describe the noisy image and estimating the original image from those features.

In this work, a 20-layer CNN to de-noise an input image is used from [27]. Utilizing both the Batch normalization and the Rectifier Linear Unit (ReLU), a feed forward convolutional Neural Network is proposed. Residual mapping is used to estimate the noise  $n$  i.e.  $R(I') \approx a$ . From this, the original image  $I(n, m)$  can be estimated using the equation 3.

$$I(n, m) = I'(n, m) - R(I') \quad (3)$$

The loss function that is minimized in this estimation is the average mean square error between the required residual images and estimated noise.

$$L(\phi) = \frac{1}{2N} \sum_{i=1}^N \|R(I'_i; \phi) - (I'_i - I_i)\|_F^2 \quad (4)$$

This loss function can be used in learning the training parameters  $\phi$  of the deep net. Here  $N$  represents the total set of clean and noisy image pairs. The Batch Normalization is used to enhance and stabilize the training performance of the network.

## 2.2. MR Image Smoothing by ADF

Another way to de-noise the observed images affected by noise is to use various diffusion techniques that de-noise the image using partial differential equations. Anisotropic diffusion is an iterative process of image diffusion using non-linear partial differential equations. Perona & Malik [11] discretised the anisotropic diffusion process using Equation 5.

$$I_{t+1}(n, m) = I_t(n, m) + \frac{\lambda}{|\mu|} \sum_{p \in \mu} g_k * (|\nabla I_{n,m,p}|) * \nabla I_{n,m,p} \quad (5)$$

Where  $I(n, m)$  represents the 2-Dimensional image,  $t$  indicates the iteration number,  $g$  is the conductance function, the constant  $\lambda$  indicates the rate of diffusion and  $\mu$  describes the four-pixel neighbourhood of pixel  $n, m$ .

## 2.3. Tumor Segmentation using Watershed Transform

Watershed transform works by assuming a grayscale image as a 3-dimensional (3D) surface and exploiting the morphological shape of the surface. In this method, the grayscale image is considered to be a 3D surface consisting of peaks (the brightness) and valleys. The watershed transform segments the image by considering it as a topological surface and finding out the watershed lines. The 3D image surface is flooded from its minima, and different sources are prevented to merge with each other by building dams. The result is a partitioned image into two main components; catchment basins and watershed lines. The algorithm stops when there are no dams to build. At the end of the algorithm, the watershed lines give the segments of the image. The watershed transform may end up over-segmenting the image due to too many minima regions. This can be solved by using markers that specify the allowed values of the regional minima. In marker based watershed transform, the image gradient magnitude is utilized as a segmentation function that generates the catchment basins having homogenous gray level and sharp watershed lines for the image segments.

The Sobel edge masks are used in the calculation of the image gradient magnitude [28]. The approximate gradient magnitude is computed using equation 6.

$$|G| = |G_n| + |G_m| \quad (6)$$

Where  $G_n$  and  $G_m$  are the Sobel convolutional kernels.

In the post processing phase of the watershed transform, different morphological techniques can be used to clean up the image. In this work, we used opening and closing operations to extract the foreground object after the transform output. In opening by reconstruction, erosion is performed on the image that shrinks the image according to the structuring element. In this paper, a structuring element in a disk shape with radius 10 is used. The objects in the image smaller than the disk are removed. The remaining objects are reconstructed to their original shape using image reconstruction. Image reconstruction uses starting seed pixels and grows them in a flooding method until the complete connected objects are obtained. In the last phase of the post processing, any dark spots left in the image are removed using morphological operation i.e. closing by reconstruction. In the closing by reconstruction, image dilation is performed according to the disk-structuring element that expands and thickens the foreground objects and removes any dark spots left in the image.

Otsu Thresholding method is used on grayscale images to convert them into binary images using an optimum threshold that separates the image into black and white pixels in such a way that the intra class variance is minimized [29]. An iterative search for the optimum threshold  $t$  having the value between 1 to  $N$  is done in this method. Where  $N$  is the maximum intensity level of the image. Intra class variance is minimized using this optimum threshold value. Intra class variance is the weighted sum of the variances of both classes.

$$\sigma_\omega^2(t) = \omega_0(t)\sigma_0^2(t) + \omega_1(t)\sigma_1^2(t) \quad (7)$$

Where  $\omega_i$  are the class probabilities and  $\sigma_i^2(t)$  are the variances of each class. Minimizing the intra class variance was found to be the similar to maximizing the inter class variance in the Otsu method. The Otsu thresholding algorithm computes the histogram and probability of each intensity level in the image. After this, probabilities and inter class variances for all possible thresholds are calculated and the optimum threshold is selected that corresponds to maximum inter class variances.

## 4. Results and Discussions

BraTS benchmarked dataset [8] is used for testing the proposed system. Medical Image Computing and Computer Assisted Intervention (MICCAI) provides this dataset available online for research. It primarily consists of LGG and HGG with four sequence types namely T1, T2, T1c and Flair. Fig. 2 shows the visual representation of five different MR images of a certain case selected as sample. The first column of the Fig. 2 shows the original MR image. The Rician noise is introduced in the image to check the efficiency of proposed denoising method as shown in column 2 of Fig. 2. The result of denoising using ADF is shown in column 3. Column 4 shows the result of denoising using Deep CNN. In the last column, the visual results of denoising using a combination of Deep CNN and ADF (Deep CNN-AD) is shown. It is clear from the images for the five cases that better image quality is secured when we apply both Deep CNN and Gaussian. The experimental results are based on 400 tumor MRI from 18 different cases.

The de-noising performance of different techniques are usually measured with Signal to Noise Ratio (SNR) and Peak Signal to Noise Ratio (PSNR) values as shown in equation 8 and 9 respectively [30]. The higher these values are the better the performance of any particular technique. In this paper, these same values will be used as the basis for comparison of the de-noising techniques.

$$SNR = 10 \log_{10} \left[ \frac{\sum \sum \Delta I_{org}(n, m)^2}{\sum \sum [\Delta I_{org}(n, m) - \Delta I_{est}(n, m)]^2} \right] \quad (8)$$

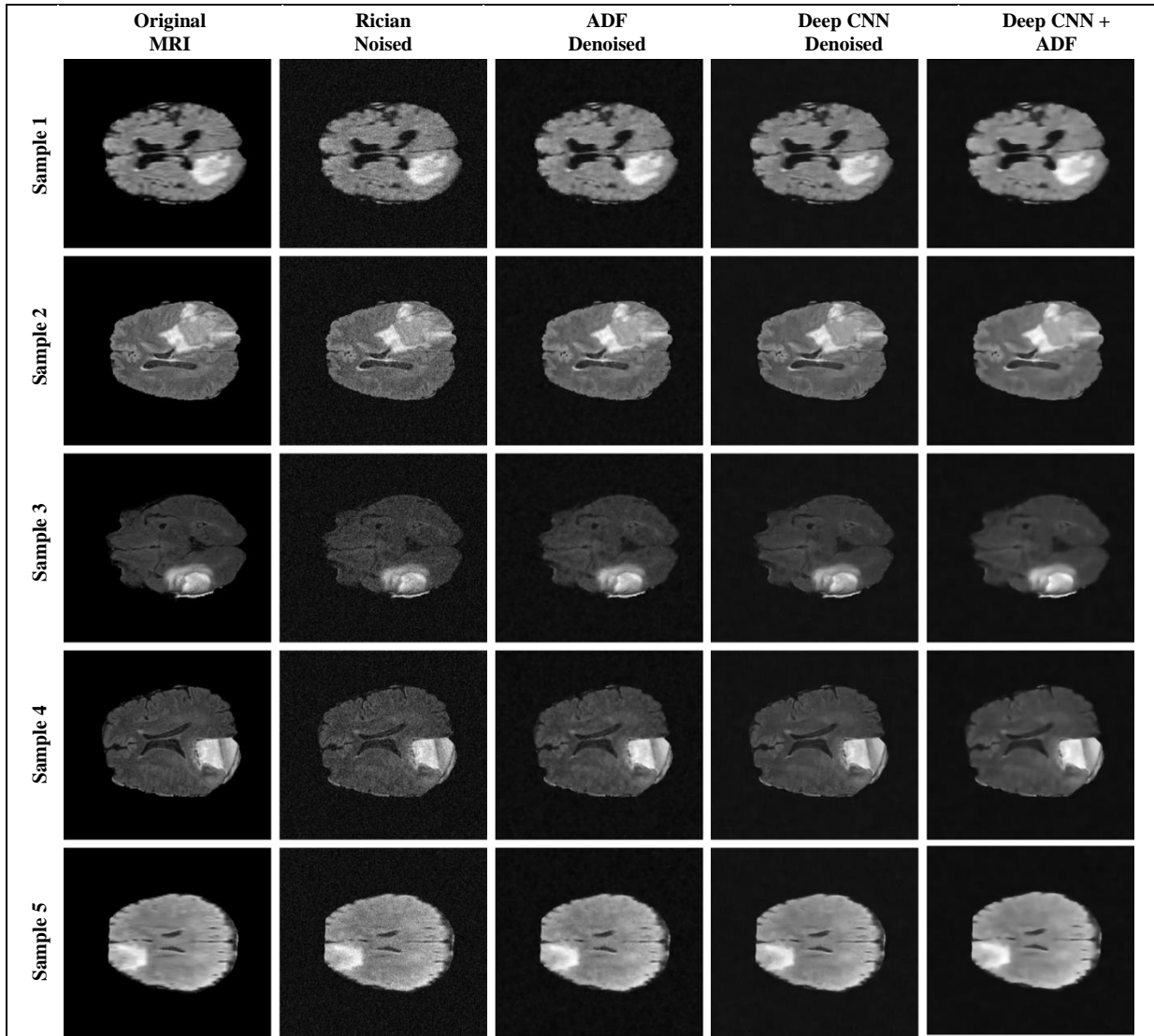


Fig. 2: Visual results of the Rician denoising of MRI Image selected samples

$$PSNR = 10 \log_{10} \left[ E \left\{ \frac{\max |I_{org}|^2}{\|I_{org} - I_{est}\|_F^2} \right\} \right] \quad (9)$$

As shown in Table 1, in all 5 samples the Deep CNN and ADF combination produced higher SNR and PSNR that each applied individually as mentioned earlier. The proposed denoising technique outperforms the Deep CNN and ADF applied separately for each sample and for all samples in the dataset.

The real test of any proposed method will depend on the sensitivity and specificity of successfully classifying and diagnosing the tumor. In order to test the performance of different techniques including the one proposed in this paper, statistical methods based on Dice Similarity Coefficients (DSC), Specificity and Sensitivity are used. The basis for these parameters is to check the number of same pixels segmented between ground truth and image. Terms associated with these parameters include True Positive (TP), False Positive (FP), True Negative (TN) and False Negative (TN). These terms analyse the performance of the segmentation portion of the techniques. When referring to Ground Truth Image, the indication is the reference image which is divided into segmented portion (foreground) black pixels and background (white pixels). Therefore, TN is number of pixels segmented correctly as background, TP is number of pixels segmented correctly as foreground, FN is number of pixels segmented incorrectly as background and FP is number of pixel segmented incorrectly as foreground. A validation

metric that measure the percentage of overlapping segmented parts of any two images in the special domain is referred to as DSC and calculated using equation 13.

Table 1: Numerical results of Deep CNN and Gaussian Rician denoising for selected samples.

Data	Method	SNR	PSNR
Sample - 1	ADF	13.841	25.352
	Deep CNN	12.376	23.887
	Deep CNN + ADF	14.495	26.006
Sample - 2	ADF	12.644	24.830
	Deep CNN	11.496	23.683
	Deep CNN + ADF	13.696	24.883
Sample - 3	ADF	8.957	25.216
	Deep CNN	7.590	23.848
	Deep CNN + ADF	9.382	25.641
Sample - 4	ADF	11.211	25.468
	Deep CNN	9.661	23.918
	Deep CNN + ADF	11.971	26.228
Sample - 5	ADF	15.207	25.718
	Deep CNN	13.254	23.765
	Deep CNN + ADF	15.821	26.632

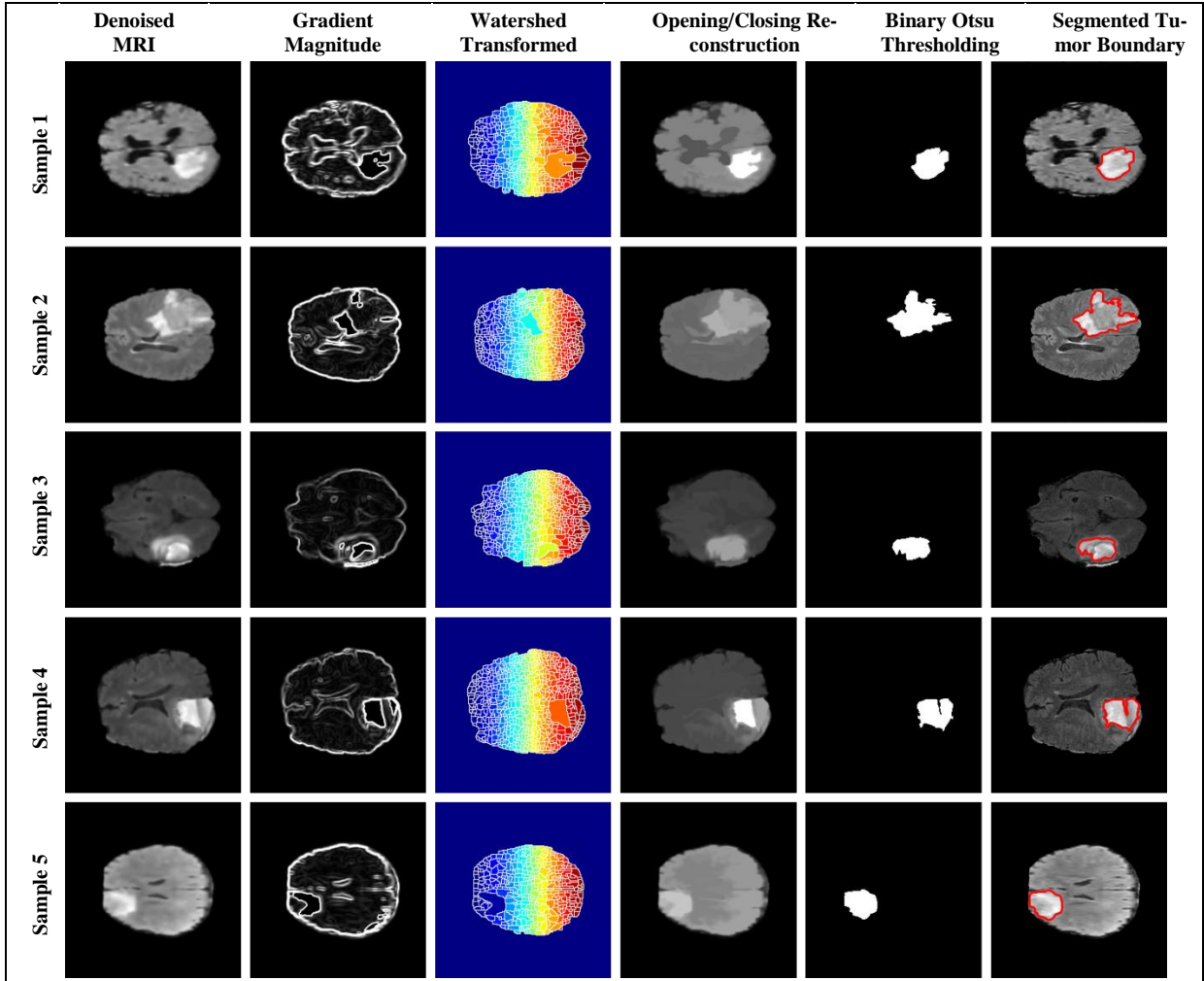


Fig. 3: Visual results of the Tumor Part Segmentation of MRI Image selected samples.

$$D(G, I) = \frac{2(G \cap I)}{(G + I)} = \frac{2 \times TP}{((FP + TP) + (TP + FN))} \quad (13)$$

Where  $G$  and  $I$  are the values of the pixels that belong to segmented foreground of ground truth image and proposed method image respectively,  $\cap$  is a logical AND operator.

Sensitivity and specificity are calculated as shown in equations 15 and 16 respectively.

$$\text{Sensitivity} = \frac{TP}{TP + FN} \quad (15)$$

$$\text{Specificity} = \frac{TN}{TN + FP} \quad (16)$$

Table 2 shows the numerical results of the watershed based segmentation method. The proposed method outperform all previous method with an average specificity of 99.85%, sensitivity of 82.85% and DSC of 90.46%. It is clear that the denoising of the image had significant effect on the accurate segmentation of the tumor portion of the image.

Fig. 3 shows the visual results for the segmentation of the tumor using the proposed technique. The resulting denoised image obtained in Fig. 2 is shown in the first column of Fig. 3. The second column in Fig. 3 shows the result of the image after applying the gradient magnitude. Watershed transform is then applied the image and the result is as shown in column 3. The opening and closing reconstruction result is shown in column 4 before applying the binary Otsu thresholding which results in the images shown in column 5. The tumor is then successfully and accurately segmented as shown in column 6.

Table 2: Numerical results of Watershed based Segmentation for the complete tumor compared with the existing methods.

Algorithm	DSC	Sensitivity	Specificity
Proposed Method	90.46%	82.85%	99.85%
Havaei 2017 [31]	88%	79%	89%
Pereira 2016 [32]	84%	86%	-
Kwon 2014 [33]	82%	83%	-
Bauer 2011 [34]	77% to 84%	-	-

## 5. Conclusion

MR images are affected by noise during the acquisition and transmission phase of MRI process. The noise affects the accurate segmentation of tumorous portion of the image. Many methods and techniques have been proposed for the denoising of the images however denoising affects the quality of the image and may in some case result in the loss of key features of the image. In this paper, a novel method was proposed for the effective denoising of the MR image while maintaining image quality and key features. The method referred to as Deep CNN-AD was effective and outperformed the Deep CNN and Gaussian when applied separately. The denoised image was then subjected to several phases including but not limited to watershed transform, opening/closing reconstruction and binary Otsu threshold in order to accurately segment the tumor portion of the image. The segmentation produced an average Specificity of 99.8598.93% and dice coefficient of 90.46%



outperforming all previous technique mentioned in previous literature.

## References

- [1] Kural, C., Pusat, S., Şentürk, T., Seçer, H.İ. and İzci, Y., (2011), "Extracranial metastases of anaplastic oligodendroglioma", *Journal of Clinical Neuroscience*, 18(1), pp.136-138.
- [2] Louis, D.N., Ohgaki, H., Wiestler, O.D., Cavenee, W.K., Burger, P.C., Jouvett, A., Scheithauer, B.W. and Kleihues, P., (2007) "The 2007 WHO classification of tumours of the central nervous system", *Acta neuropathologica*, 114(2), pp.97-109.
- [3] Van Meir, E.G., Hadjipanayis, C.G., Norden, A.D., Shu, H.K., Wen, P.Y. and Olson, J.J., (2010), "Exciting new advances in neuro-oncology: The avenue to a cure for malignant glioma", *CA: a cancer journal for clinicians*, 60(3), pp.166-193.
- [4] Link, M.J. and Perry, A., (2009), "Meningioma Tumorigenesis: An Overview of Etiologic Factors", In *Meningiomas* (pp. 137-145). Springer London.
- [5] Nag, M.K., Koley, S., Chakraborty, C. and Sadhu, A.K., (2015), "Magnetic Resonance Image Quality Enhancement Using Transform Based Hybrid Filtering", In *Advancements of Medical Electronics* (pp. 39-48). Springer, New Delhi.
- [6] Garg, S. and Kaur, J., (2013), "Improving segmentation by denoising brain MRI image through interpolation median filter in ADTVFCM", *International Journal of Computer Trends and Technology*, 4(2), pp.187-188.
- [7] Khan, A., Alasad, J. and Latif, G., (2017), "Speckle Suppression in Medical Ultrasound Images through Schur Decomposition", *IET Image Processing*.
- [8] Menze, B.H., Jakab, A., Bauer, S., Kalpathy-Cramer, J., Farahani, K., Kirby, J., Burren, Y., Porz, N., Slotboom, J., Wiest, R. and Lanczi, L., (2015), "The multimodal brain tumor image segmentation benchmark (BRATS)", *IEEE transactions on medical imaging*, 34(10), pp.1993-2024. Vancouver
- [9] Balafar, M.A., Ramli, A.R., Saripan, M.I. and Mashohor, S., (2010), "Review of brain MRI image segmentation methods", *Artificial Intelligence Review*, 33(3), pp.261-274.
- [10] M.A .Balafar, (2012), "Review of noise reducing algorithms for brain MRI images", *International Journal on Technical and Physical Problems of Engineering*, Published by International Organization of IOTPE, Vol.4, Issue 13, No. 4, pp 54-59.
- [11] Perona, P. and Malik, J., (1990), "Scale-space and edge detection using anisotropic diffusion", *IEEE Transactions on pattern analysis and machine intelligence*, 12(7), pp.629-639.
- [12] Jaffar, M. A., Zia, S., Latif, G., Mirza, A. M., Mehmood, I., Ejaz, N., & Baik, S. W. (2012), "Anisotropic diffusion based brain MRI segmentation and 3D reconstruction", *International Journal of Computational Intelligence Systems*, 5(3), 494-504.
- [13] Luisier, F. and Wolfe, P.J., (2011), "Chi-square unbiased risk estimate for denoising magnitude MR images", In *Image Processing (ICIP), 2011 18th IEEE International Conference on* (pp. 1561-1564). IEEE.
- [14] Buades, A., Coll, B. and Morel, J.M., (2005), "A non-local algorithm for image denoising", In *Computer Vision and Pattern Recognition, 2005. CVPR 2005. IEEE Computer Society Conference on* (Vol. 2, pp. 60-65). IEEE.
- [15] Tomasi, C. and Manduchi, R. (1998), "Bilateral filtering for gray and color images", In *Proceedings of the sixth international conference on computer vision*, pp 839-846.
- [16] Prima, S. and Comowick, O., (2013), "Using bilateral symmetry to improve non-local means denoising of MR brain images", In *Biomedical Imaging (ISBI), 2013 IEEE 10th International Symposium on* (pp. 1231-1234). IEEE.
- [17] Golshan, H.M. and Hasanzadeh, R.P., (2013), "A modified Rician LMMSE estimator for the restoration of magnitude MR images", *Optik-International Journal for Light and Electron Optics*, 124(16), pp.2387-2392.
- [18] Manjón, J.V., Coupé, P., Buades, A., Collins, D.L. and Robles, M., (2012), "New methods for MRI denoising based on sparseness and self-similarity", *Medical image analysis*, 16(1), pp.18-27.
- [19] Zhang, C., Hu, W., Jin, T. and Mei, Z., (2016), "Nonlocal image denoising via adaptive tensor nuclear norm minimization", *Neural Computing and Applications*, pp.1-17.
- [20] Sharif, M., Hussain, A., Jaffar, M.A. and Choi, T.S., (2015), "Fuzzy similarity based non local means filter for rician noise removal", *Multimedia tools and applications*, 74(15), pp.5533-5556.
- [21] Pinheiro, P. and Collobert, R., (2014), "Recurrent convolutional neural networks for scene labeling", In *International Conference on Machine Learning*, pp. 82-90.
- [22] Farabet, C., Couprie, C., Najman, L. and LeCun, Y., (2013), "Learning hierarchical features for scene labeling", *IEEE transactions on pattern analysis and machine intelligence*, 35(8), pp.1915-1929.
- [23] Long, J., Shelhamer, E. and Darrell, T., (2015), "Fully convolutional networks for semantic segmentation", In *Proceedings of the IEEE Conference on Computer Vision and Pattern Recognition*, pp. 3431-3440.
- [24] Havaei, M., Davy, A., Warde-Farley, D., Biard, A., Courville, A., Bengio, Y., Pal, C., Jodoin, P.M. and Larochelle, H., (2017), "Brain tumor segmentation with deep neural networks", *Medical image analysis*, 35, pp.18-31.
- [25] Gauch, J.M., (1999), "Image segmentation and analysis via multiscale gradient watershed hierarchies", *IEEE transactions on image processing*, 8(1), pp.69-79.
- [26] Pal, C., Das, P., Chakrabarti, A., & Ghosh, R., (2017), "Rician noise removal in magnitude MRI images using efficient anisotropic diffusion filtering", *International Journal of Imaging Systems and Technology*, 27(3), 248-264.
- [27] Zhang, K., Zuo, W., Chen, Y., Meng, D., & Zhang, L., (2017), "Beyond a gaussian denoiser: Residual learning of deep cnn for image denoising", *IEEE Transactions on Image Processing*.
- [28] Gao, W., Zhang, X., Yang, L., & Liu, H., (2010), "An improved Sobel edge detection", In *3rd International Conference on Computer Science and Information Technology (ICCSIT)*, Vol. 5, pp. 67-71, IEEE.
- [29] Latif, G., Iskandar, D. A., Jaffar, A., & Butt, M. M. (2017). Multimodal Brain Tumor Segmentation using Neighboring Image Features. *Journal of Telecommunication, Electronic and Computer Engineering (JTEC)*, 9(2-9), 37-42.
- [30] Wiest-Daesslé, N., Prima, S., Coupé, P., Morrissey, S. P., & Barillot, C., (2008), "Rician noise removal by non-local means filtering for low signal-to-noise ratio MRI: applications to DT-MRI", In *International Conference on Medical Image Computing and Computer-assisted Intervention*, pp. 171-179. Springer, Berlin, Heidelberg.
- [31] Havaei, M., Davy, A., Warde-Farley, D., Biard, A., Courville, A., Bengio, Y., ... & Larochelle, H., (2017), "Brain tumor segmentation with deep neural networks", *Medical image analysis*, 35, pp. 18-31.
- [32] Pereira, S., Pinto, A., Alves, V., & Silva, C. A. (2016), "Brain tumor segmentation using convolutional neural networks in MRI images", *IEEE transactions on medical imaging*, 35(5), pp. 1240-1251.
- [33] Kwon, D., Shinohara, R. T., Akbari, H., & Davatzikos, C., (2014), "Combining generative models for multifocal glioma segmentation and registration", In *International Conference on Medical Image Computing and Computer-Assisted Intervention* (pp. 763-770). Springer, Cham.
- [34] Bauer, S., Nolte, L. P., & Reyes, M., (2011), "Fully automatic segmentation of brain tumor images using support vector machine classification in combination with hierarchical conditional random field regularization", In *International Conference on Medical Image Computing and Computer-Assisted Intervention* (pp. 354-361). Springer, Berlin, Heidelberg.